Chinese Chemical Letters 34 (2023) 107906

Contents lists available at ScienceDirect

Chinese Chemical Letters

journal homepage: www.elsevier.com/locate/cclet

Toehold-mediated strand displacement reaction-propelled cascade DNAzyme amplifier for microRNA let-7a detection

Na Wang[a,1], Yongjian Jiang[a,1], Kunhan Nie[a], Di Li[b], Hui Liu[a], Jian Wang[a], Chengzhi Huang[a], Chunmei Li[a,*]

[a] Key Laboratory of Luminescence Analysis and Molecular Sensing (Southwest University), Ministry of Education, College of Pharmaceutical Sciences, Southwest University, Chongqing 400715, China
[b] The Second Affiliated Hospital of Chongqing Medical University, Chongqing 400010, China

ARTICLE INFO

Article history:
Received 13 June 2022
Revised 4 October 2022
Accepted 14 October 2022
Available online 17 October 2022

Keywords:
DNAzyme amplifier
Toehold-mediated strand displacement reaction
Signal amplification
let-7a
Cancer marker

ABSTRACT

DNAzyme amplifiers have been extensively explored as a useful sensing platform, but single DNAzyme amplifier is limited in biosensing applications by its low sensitivity. Herein, a cascade DNAzyme amplifier was designed by exploiting concurrent amplification cycle principles of toehold-mediated strand displacement reaction (TSDR) and Zn^{2+}-assisted DNAzyme cycle with lower cost and simpler procedures. Compared with single DNAzyme amplifier, the proposed TSDR-propelled cascade DNAzyme amplifier exhibited higher sensitivity by releasing more DNAzyme through TSDR to cleave substrate strand during the DNAzyme cycle. Base on this, let-7a could be sensitively detected in the range of 5–50 nmol/L with a detection limit of 64 pmol/L. Furthermore, the dual signal amplification strategy of the cascade DNAzyme amplifier exhibited excellent selectivity to distinguish single-base mismatched DNA strands, which has been successfully applied to the determination of let-7a in blood serum, showing high promise in early cancer diagnosis.

MicroRNA (miRNA) is a gene expression regulator, which mainly mediates transcription and post-transcriptional control of target gene expression [1–5]. Among them, let-7 miRNA, as a time regulator of cell development, was first discovered in caenorhabditis elegans [6,7]. It is noteworthy that let-7a is an important tumor suppressor and cancer marker in the let-7 miRNA family, which has extremely important clinical significance [8]. Recent studies have also shown that the abnormal expression of let-7a is closely related to cell proliferation and apoptosis [9]. Therefore, a series of let-7a detection methods have been reported, including surface-enhanced Raman scattering [10], electrochemistry [11,12], colorimetry [13] and fluorescence [14,15]. Among these detection methods, fluorescence is considered as one of the most attractive technologies [16,17]. Furthermore, fluorescent probes based on fluorescence resonance energy transfer (FRET) has been widely used in the fields of biomarkers analysis with the advantages of simple operation, low background signal and intuitive accuracy [18–21]. However, owing to the natural characteristics of small size and low abundance, signal amplification is often required to effectively detect let-7a with improved detection sensitivity [22].

DNAzyme, a kind of DNA strand that mimics the function of protease, can be activated under the regulation of specific stimuli to exert their effects [23–25]. Comparing to protein enzymes and RNA enzymes, DNAzyme is easier to synthesize, more stable and less expensive [26,27]. Therefore, by taking advantage of the catalytic properties, DNAzyme has been wildly used as a signal amplification medium to construct DNAzyme amplifiers for various biomarkers detection [28–30]. However, owing to the low catalytic activity of DNAzyme alone on substrates, these traditional DNAzyme amplifiers with low sensitivity were hard to fulfill the application in biosensing and early diagnosis of cancer [31].

To further improve the sensitivity of DNAzyme amplifier, a variety of cascade DNAzyme amplifiers have been assembled by exploiting concurrent amplification cycle principles of DNAzyme and nuclease, such as exonuclease-mediated target recycling [32], nicking endonuclease cleavage [33] and polymerase extension [34]. Though these methods have high sensitivity, most of them are limited by the higher testing costs and cumbersome procedures [35]. At present, DNA-based signal amplification strategies, such as loop-mediated isothermal amplification [36], hyperbranched rolling circle amplification [37] and toehold-mediated strand displacement

* Corresponding author.
E-mail address: licm1024@swu.edu.cn (C. Li).
[1] These authors contributed equally to this work.

https://doi.org/10.1016/j.cclet.2022.107906
1001-8417/

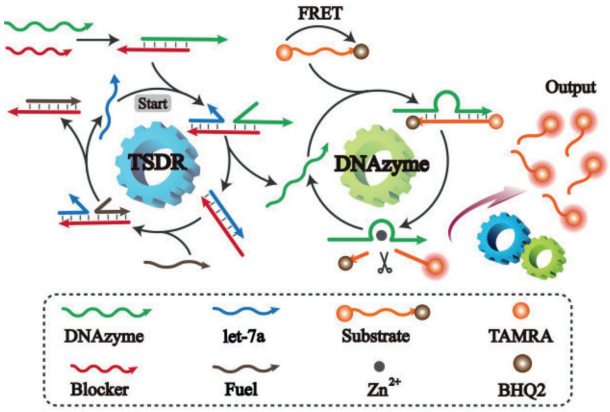

Scheme 1. Schematic diagram of the TSDR-propelled cascade DNAzyme amplifier for let-7a detection.

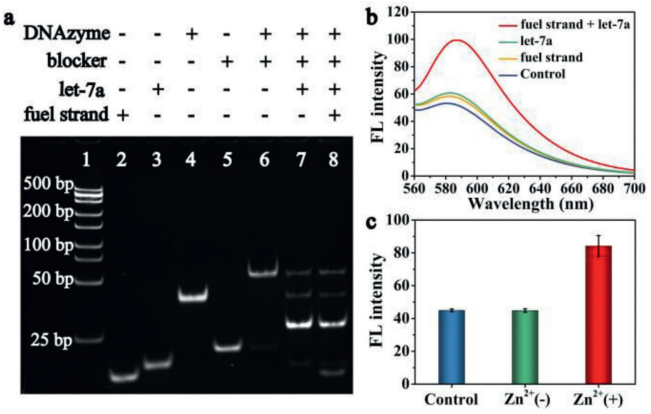

Fig. 1. Characterization of the TSDR-propelled cascade DNAzyme amplifier. (a) Native PAGE (12%) analysis. Lanes 1–8: DNA marker, fuel strand, DNA let-7a, DNAzyme, blocker, DNAzyme + blocker, DNAzyme-blocker + let-7a, DNAzyme-blocker + let-7a + fuel strand. (b) Fluorescence spectra of the TSDR-propelled cascade DNAzyme amplifier. Concentrations: DNAzyme, 25 nmol/L; blocker, 30 nmol/L; fuel strand, 50 nmol/L; substrate strand, 50 nmol/L; Zn^{2+}, 1.25 mmol/L; let-7a, 10 nmol/L. Time: 30 min. Temperature: 37 °C. (c) The fluorescence response of DNAzyme cycle. Control represented that only the substrate strand and Zn^{2+} were present in the system. $Zn^{2+}(-)$ represented the presence of substrate strand and DNAzyme without Zn^{2+} in the system. $Zn^{2+}(+)$ represented that substrate strand, DNAzyme and Zn^{2+} were all present in the system. Concentrations: DNAzyme, 25 nmol/L; substrate strand, 50 nmol/L; Zn^{2+}, 1.25 mmol/L. Time: 30 min. Temperature: 37 °C.

reaction (TSDR) [38], have been extensively studied. Among them, as a nonenzymatic signal amplification process that can occur at room temperature, TSDR have been emerged as a powerful strategy for biomarkers recognition with high signal gains [39,40]. More importantly, combining TSDR with the DNAzyme amplifiers can effectively release more DNAzymes to cut more substrates during the DNAzyme cycle, thus achieving dual signal amplification with higher sensitivity, lower cost and simpler procedures.

Herein, a TSDR-propelled cascade DNAzyme amplifier was assembled by exploiting concurrent amplification cycle principles of TSDR and DNAzyme (Scheme 1). At the beginning, the fluorescence of tetramethyl rhodamine (TAMRA) in the substrate strand could be effectively quenched by black hole quencher 2 (BHQ2) based on FRET. Besides, DNAzyme activity is first inhibited after the hybridization with blocker DNA, which can be competed in the presence of target let-7a, resulting in the release of DNAzyme for recognizing the active site of the substrate strand and cutting it. Subsequently, the fuel strand can bind to the blocker in the double stranded DNA (dsDNA) to cyclically release the target let-7a by utilizing TSDR, resulting in more DNAzymes to be released to realize the first amplification. Furthermore, on the basis of second signal amplification driven by Zn^{2+}-assisted DNAzyme amplifiers, these released DNAzymes by TSDR can cyclically cleave the substrate strand, leading to higher fluorescence recovery of TAMRA, thus achieving dual signal amplification with lower cost and simpler procedures. Based on this, the sensitivity of let-7a detection was effectively improved by the TSDR-propelled cascade DNAzyme amplifier compared to single DNAzyme amplifier.

Firstly, the TSDR was verified by the native polyacrylamide gel electrophoresis (PAGE) (Fig. 1a). Lane 1 was the DNA marker and Lanes 2-5 were fuel strand, DNA let-7a, DNAzyme and blocker, respectively. Compared with Lanes 4 and 5, the migration rate of Lane 6 was slower, indicating the successful hybridization of DNAzyme and blocker. Besides, both Lanes 7 and 8 showed a band corresponding to Lane 4, which was the released DNAzyme. Since blocker-target let-7a and blocker-fuel strand have similar molecular weight, the feasibility of the TSDR was further verified by fluorescence spectra. The distance between TAMRA and BHQ2 modified at both ends of the substrate strand was less than 10 nm, so that the fluorescence of TAMRA in the substrate strand could be effectively quenched by BHQ2 based on FRET. On the other hand, the DNAzyme activity in the dsDNA formed by blocker hybridization with DNAzyme was blocked. At this point, DNAzyme could not recognize and cut the substrate strand, thus TAMRA fluorescence was low (Fig. 1b). Compared with the addition of let-7a alone, the fluorescence recovery of TAMRA was higher after further introduction of fuel strand. This revealed that the introduction of fuel strand could successfully trigger TSDR, so as to cyclically release more DNAzyme for substrate cutting, which proved that the DNA sequence design of TSDR was reasonable. It is worth noting that the fluorescence of TAMRA hardly recovered when only the fuel strand was present, indicating that the fuel strand could not replace the DNAzyme in the dsDNA formed by blocker and DNAzyme to start the DNAzyme cycle, thus confirming the stability of the TSDR. In addition, when only DNAzyme and substrate strand were present, the fluorescence of TAMRA hardly recovered in the absence of Zn^{2+} compared with that in the presence of Zn^{2+}, demonstrating that DNAzyme cycle could run smoothly with the assistance of Zn^{2+} (Fig. 1c).

The dual signal amplification in let-7a detection of the cascade DNAzyme amplifier was further explored. In the single DNAzyme amplifier lacking fuel strand, one let-7a strand could only displace one DNAzyme strand since the binding force between let-7a and blocker was stronger than that between the DNAzyme and blocker, resulting in low fluorescence recovery efficiency (Figs. 2a and b). Nevertheless, after further introducing the fuel strand into the system to construct TSDR-propelled cascade DNAzyme amplifier, let-7a can be replaced from dsDNA through strand displacement reaction, thus resulting in more DNAzyme release. These released DNAzymes by TSDR were cyclically cleaving the substrate strand and releasing more TAMRA, which led to higher fluorescence recovery (Figs. 2c and d). In addition, the fluorescence lifetime of TAMRA recovered from 2.00 ns to 3.46 ns when let-7a was added into the cascade DNAzyme amplifier, proving that the substrate strand was successfully cut by the release of DNAzyme trigged by the presence of let-7a, which further provide the potential for the detection of let-7a by the TSDR-propelled cascade DNAzyme amplifier (Fig. S1 in Supporting information).

To achieve suitable analytical performance, the key conditions of the cascade DNAzyme amplifier such as the ratio of DNAzyme to blocker, the length and concentration of fuel strand, the ratio of DNAzyme to substrate strand were optimized. The fluorescence recovery efficiency of $(F-F_0)/F_0$ was calculated to evaluate the optimal conditions, where F and F_0 represented the fluorescence intensities of TAMRA at 585 nm with and without let-7a, respectively.

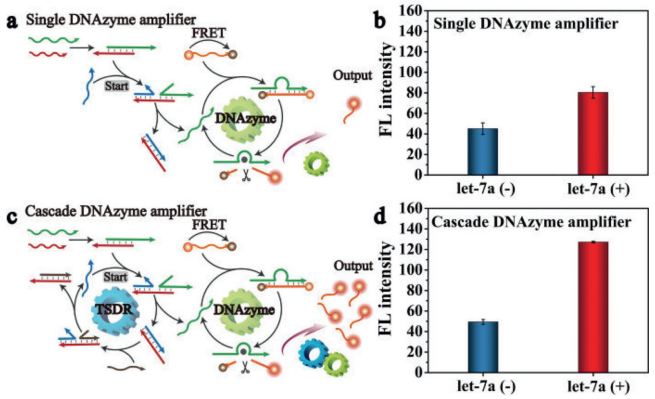

Fig. 2. Comparison of the single DNAzyme amplifier and cascade DNAzyme amplifier in let-7a detection. (a, b) Schematic diagram and fluorescence response for the detection of let-7a by the single DNAzyme amplifier. (c, d) Schematic diagram and fluorescence response for the detection of let-7a by the cascade DNAzyme amplifier. let 7a (+) and let 7a (−) represented the presence and absence of let-7a in the system, respectively. Concentrations: DNAzyme, 25 nmol/L; blocker, 30 nmol/L; fuel strand, 50 nmol/L; substrate strand, 50 nmol/L; Zn^{2+}, 1.25 mmol/L; let-7a, 40 nmol/L; time: 30 min; temperature: 37 °C. Each measurement was performed in triplicate (error bars indicate standard deviation).

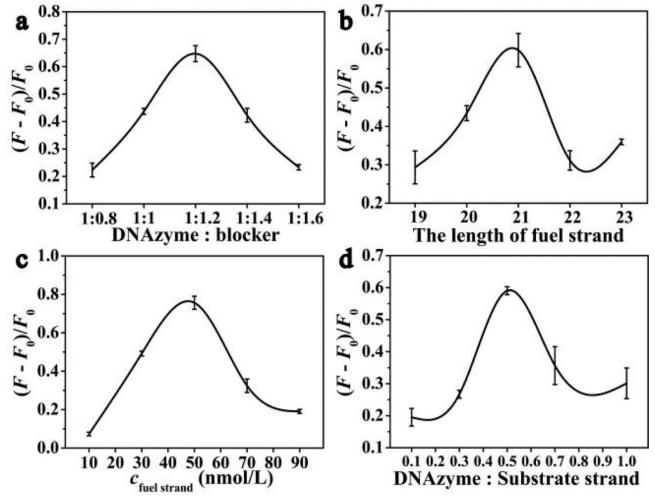

Fig. 3. Experimental conditions optimization for the detection of let-7a. (a) The ratio of DNAzyme to blocker, (b) the length of fuel strand, (c) fuel strand concentration and (d) the ratio of DNAzyme to substrate strand on the let-7a detection. Concentrations: DNAzyme, 25 nmol/L; blocker, 30 nmol/L; fuel strand, 50 nmol/L; substrate strand, 50 nmol/L; Zn^{2+}, 1.25 mmol/L; let-7a, 10 nmol/L; time: 30 min; temperature: 37 °C. Each measurement was performed in triplicate (error bars indicate standard deviation).

Firstly, the ratio of DNAzyme to blocker determines the degree of blocking of DNAzyme activity. When the amount of DNAzyme in the solution was more than that of blocker, free DNAzyme can cleave the substrate without the presence of let-7a, which caused the background signal too high. Nevertheless, when the amount of blocker in the solution was too large, free blocker can preferentially compete for let-7a, resulting in low detection sensitivity. When the ratio of DNAzyme and blocker was 1:1.2, the signal recovery reached the maximum value (Fig. 3a). Then, the length and concentration of fuel strand played an important role on triggering the release of target let-7a by TSDR. It was found that when the fuel strand was too short, it cannot compete with let-7a for the blocker. If the fuel strand was too long, it would bind to the blocker and release DNAzyme even if there was no let-7a. Therefore, a fuel strand with a length of 21 bases was selected for subsequent experiments (Fig. 3b). And the concentration of the fuel strand was chosen as 50 nmol/L to obtain an obvious change in the fluorescent signal (Fig. 3c). In addition, DNAzyme was selected to cut the substrate strand to generate the signal and the relationship between the number of DNAzyme and the substrate strand played an important role in the fluorescent signal recovery. Based on this, we found when the ratio between the DNAzyme and the substrate strand reached 0.5:1, the signal recovery value was the highest (Fig. 3d). At last, effects of the experimental conditions including Zn^{2+} concentration, incubation temperature and time on detection let-7a were also explored. The assistance of Zn^{2+} is very important to DNAzyme for recognizing the active site of substrate strand and cutting it. In the case of Zn^{2+} concentration of 1.25 mmol/L, DNAzyme had a better cutting effect on the substrate, resulting in a higher fluorescence recovery (Fig. S2a in Supporting information). Besides, the reaction conditions were optimized as incubation with let-7a at 37 °C for 30 min before fluorescence measurement (Figs. S2b and c in Supporting information).

Under the above optimal conditions, the capability of the cascade DNAzyme amplifier for the detection of let-7a was identified by comparing the single signal amplification and dual signal amplification strategies. As the concentration of let-7a increased, the fluorescence of TAMRA gradually increased when there was no fuel strand in the system (Fig. 4a). The $(F-F_0)/F_0$ value and let-7a concentration showed a good linear relationship with the linear regression equation of $(F-F_0)/F_0 = 0.0131c_{let\text{-}7a} + 0.184$ ($R^2 = 0.984$). The linear range of the single DNAzyme amplifier driven by DNAzyme was 10–80 nmol/L and the detection limit was 794 pmol/L (Fig. 4b). In contrast, in the dual signal amplification system of TSDR and DNAzyme cycle, as let-7a concentration gradually increased from 5 nmol/L to 50 nmol/L, the fluorescence signal was gradually increasing (Fig. 4c). The $(F-F_0)/F_0$ value and let-7a concentration showed a good linear relationship and the linear regression equation was $(F-F_0)/F_0 = 0.0238c_{let\text{-}7a} + 0.256$ ($R^2 = 0.988$), with the detection limit of 64 pmol/L (Fig. 4d), which was reduced about 12 times comparing to the single signal amplification strategy. Furthermore, compared with other miRNA let-7a detection methods, the sensitivity and the detection time of the cascade DNAzyme amplifier were also comparable to that in previous works (Table S1 in Supporting information).

Then the selectivity of the cascade DNAzyme amplifier for let-7a detection was evaluated by discrimination with other four

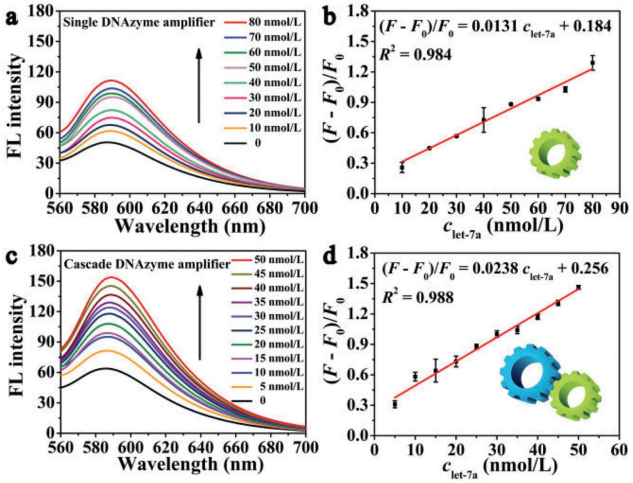

Fig. 4. Fluorescence spectra of the detection of let-7a by the single DNAzyme amplifier (a, b) and by the cascade DNAzyme amplifier (c, d). Concentrations: DNAzyme, 25 nmol/L; blocker, 30 nmol/L; fuel strand, 50 nmol/L; substrate strand, 50 nmol/L; Zn^{2+}, 1.25 mmol/L. Time: 30 min. Temperature: 37 °C. Each measurement was performed in triplicate (error bars indicate standard deviation).

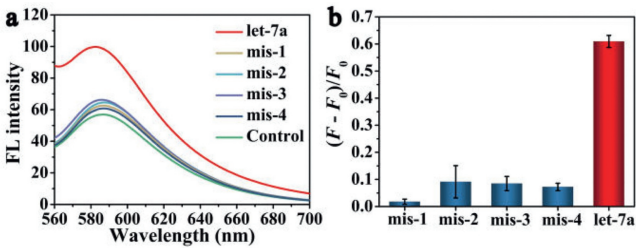

Fig. 5. Specificity of let-7a detection. (a) Fluorescence spectra of specificity detection of let-7a. (b) $(F-F_0)/F_0$ histogram of specificity detection of let-7a. Concentrations: DNAzyme, 25 nmol/L; blocker, 30 nmol/L; fuel strand, 50 nmol/L; substrate strand, 50 nmol/L; Zn^{2+}, 1.25 mmol/L; let-7a and other four mismatched miRNA,10 nmol/L. Time: 30 min. Temperature: 37 °C. Each measurement was performed in triplicate (error bars indicate standard deviation).

Table 1
Detection of let-7a in the serum samples. Concentrations: DNAzyme, 25 nmol/L; blocker, 30 nmol/L; fuel strand, 50 nmol/L; substrate strand, 50 nmol/L; Zn^{2+}, 1.25 mmol/L; let-7a, 10, 20, 40 nmol/L. Time: 30 min. Temperature: 37 °C.

Sample	Added (nmol/L)	Found (nmol/L) Mean[a] ± SD[b]	Recovery (%) ($n=3$)	RSD (%) ($n=3$)
1	10	10.0 ± 0.56	100.1	7.0
	20	19.1 ± 0.19	95.8	1.3
	40	38.3 ± 0.27	95.7	0.89
2	10	9.59 ± 0.35	95.9	3.6
	20	19.2 ± 0.38	96.0	2.0
	40	38.2 ± 0.44	94.6	1.2

[a] The mean of three determinations.
[b] SD = standard deviation.

mismatched miRNA sequences with high homology at the same concentrations. Compared with the target let-7a, the changes of fluorescence signal triggered by one-base-mismatched (mis-1), two-base-mismatched (mis-2), three-base-mismatched (mis-3) and four-base-mismatched (mis-4) were much lower than those triggered by let-7a (Figs. 5a and b), which could be attributed to the high stability of the TSDR, indicating the excellent selectivity of the cascade DNAzyme amplifier even to single-base mismatched DNA strands.

To verify the application potentiality of the cascade DNAzyme amplifier in clinical diagnosis, the approach was used to detect let-7a in human serum samples (Table 1). The let-7a concentrations measured in the spiked serum samples were statistically close to the added let-7a concentrations with recoveries from 94.6% to 100.1% and the relative standard deviation (RSD) was between 0.89% and 7.0%. A comparison of miRNA detection in real samples between this assay and previous work was displayed (Table S2 in Supporting information), showing that the proposed method could achieve sensitive and rapid detection of miRNA in blood serum. The results indicated that this approach was potential to be employed for the detection of let-7a in human serum samples, which provided new strategies for the early cancer diagnosis that was related to let-7a level.

In summary, a TSDR-propelled cascade DNAzyme amplification strategy was proposed by exploiting concurrent amplification cycle principles, which displays high sensitivity, low cost and simple procedures with the detection limit reduced about 12 times comparing to the single DNAzyme amplifier. Furthermore, the dual signal amplification strategy exhibits excellent selectivity to distinguish single-base mismatched DNA strands and satisfied recovery in complex biological samples. This combination design of target-trigged strand displacement reaction and Zn^{2+}-assisted DNAzyme cycle can further realize the universal amplification of detection signal only by changing the corresponding base sequence, which shows high promise for expanding the application of DNAzyme in low abundance biomarker detection for early cancer diagnosis.

Declaration of competing interest

The authors declare that they have no known competing financial interests or personal relationships that could have appeared to influence the work reported in this paper.

Acknowledgments

This work was financially supported by the National Natural Science Foundation of China (NSFC, Nos. 22074124 and 22134005), the fund of Fundamental Research Funds for the Central Universities (No. XDJK2020TY001), Chongqing Talents Program for Outstanding Scientists (No. cstc2021ycjh-bgzxm0178) and the Chongqing Graduate Student Scientific Research Innovation Project (No. CYB21119).

Supplementary materials

Supplementary material associated with this article can be found, in the online version, at doi:10.1016/j.cclet.2022.107906.

References

[1] J. Li, J.L. Wang, S.Y. Liu, et al., Angew. Chem. Int. Ed. 59 (2020) 20104–20111.
[2] R. Garcia-Martin, G. Wang, B.B. Brandao, et al., Nature 601 (2022) 446–451.
[3] M. Hou, D.G. He, H.Z. Wang, et al., Chin. Chem. Lett. 33 (2022) 3183–3187.
[4] J. Hu, M.H. Liu, C.Y. Zhang, Chem. Sci. 9 (2018) 4258–4267.
[5] Q. Zhang, Y. Han, C.C. Li, et al., Chem. Commun. 58 (2022) 5538–5541.
[6] M. Cevec, C. Thibaudeau, J. Plavec, Nucleic Acids Res. 38 (2010) 7814–7821.
[7] W.M. Liu, R.R. Cheng, Z.R. Niu, et al., Sci. Adv. 6 (2020) e7070.
[8] Y.S. Kim, H.J. Nam, C.Y. Han, et al., Hepatology 73 (2021) 1307–1326.
[9] Y. Yu, L. Liao, B.Y. Shao, et al., Mol. Ther. 25 (2017) 480–493.
[10] X.J. Luo, J.T. Zhu, W.Y. Jia, et al., ACS Appl. Mater. Interfaces 13 (2021) 18301–18313.
[11] M. Daneshpour, B. Karimi, K. Omidfar, Biosens. Bioelectron. 109 (2018) 197–205.
[12] W.Y. Nie, Q. Wang, L.Y. Zou, et al., Anal. Chem. 90 (2018) 12584–12591.
[13] W.W. Chen, X.B. Zhang, J.J. Li, et al., Anal. Chem. 92 (2020) 2714–2721.
[14] X.T. Shen, Y. Zhang, J.H. Sun, et al., Chem. Sci. 10 (2019) 6113–6119.
[15] C.C. Li, J.P. Hu, X.R. Zou, X.L. Luo, C.Y. Zhang, Anal. Chem. 94 (2022) 1882–1889.
[16] P.J.J. Huang, J.W. Liu, J. Anal. Test. 6 (2021) 20–27.
[17] Q. Zhang, C.C. Li, F. Ma, X.L. Luo, C.Y. Zhang, Biosens. Bioelectron. 213 (2022) 114447.
[18] D. Giust, M.I. Lucio, A.H. El-Sagheer, et al., ACS Nano 12 (2018) 6273–6279.
[19] C. Xing, S. Chen, Q.T. Lin, et al., Nanoscale 14 (2022) 1327–1332.
[20] Y.J. Jiang, N. Wang, F. Cheng, et al., Anal. Chem. 92 (2020) 11565–11572.
[21] M.K. Fan, C.Z. Huang, J. Anal. Test. 5 (2021) 195–196.
[22] T.L. Kang, J.T. Zhu, X.J. Luo, et al., Anal. Chem. 93 (2021) 2519–2526.
[23] Y.T. Xu, Y.F. Ruan, H.Y. Wang, et al., Small 17 (2021) e2100503.
[24] Z.L. Yang, K.Y. Loh, Y.T. Chu, et al., J. Am. Chem. Soc. 140 (2018) 17656–17665.
[25] K. Quan, J. Li, J.L. Wang, et al., Chem. Sci. 10 (2019) 1442–1449.
[26] Y.J. Wang, K. Nguyen, R.C. Spitale, J.C. Chaput, Nat. Chem. 13 (2021) 319–326.
[27] H.D. Qi, Y.W. Xu, P. Hu, C. Yao, D.Y. Yang, Chin. Chem. Lett. 33 (2022) 1131–1140.
[28] W. Yun, H.X. Zhong, S. Zheng, R.Q. Wang, L.Z. Yang, Sens. Actuator B: Chem. 277 (2018) 456–461.
[29] Q.T. Lin, J.Y. Wu, L.L. Jiang, et al., Analyst 147 (2022) 262–267.
[30] J. Huang, W.J. Ma, H.H. Sun, et al., ACS Appl. Bio Mater. 3 (2020) 2779–2795.
[31] Y.J. Zhou, S.S. Yu, J.H. Shang, et al., Anal. Chem. 92 (2020) 15069–15078.
[32] J.F. Pan, Y. He, Z. Liu, J.H. Chen, Chem. Commun. 57 (2021) 1125–1128.
[33] X.J. Cui, R.G. Li, X.F. Liu, et al., Anal. Chim. Acta 997 (2018) 1–8.
[34] S.T. Li, Y. Zhang, J.J. Tian, W.T. Xu, Food Chem. 324 (2020) e126859.
[35] S.F. Liu, C.B. Cheng, T. Liu, et al., Biosens. Bioelectron. 63 (2015) 99–104.
[36] J.A. Hambalek, J.E. Kong, C. Brown, et al., ACS Sens. 6 (2021) 3242–3252.
[37] M.Q. Huang, E.H. Xiong, Y. Wang, et al., Nat. Commun. 13 (2022) e968.
[38] Y.J. Jiang, X.J. Yang, J. Wang, et al., Analyst 146 (2021) 7187–7193.
[39] X.Y. Wang, Y.F. Li, S.Z. Lv, S. Bi, J. Anal. Test. 6 (2022) 12–19.
[40] F. Ma, Q. Zhang, C.Y. Zhang, Nano Lett. 19 (2019) 6370–6376.